New Continuous Mass-lumped Finite Elements for 3D Wave Propagation

Geevers, S.; Mulder, Wim; van der Vegt, J

DOI
10.3997/2214-4609.201800964

Publication date
2018

Document Version
Accepted author manuscript

Published in
80th EAGE Conference and Exhibition 2018, 11-14 June, Copenhagen, Denmark

New continuous mass-lumped finite elements for 3D wave propagation

S. Geevers
Department of Applied Mathematics, University of Twente, Enschede, the Netherlands
W.A. Mulder
Shell GSI BV & Delft University of Technology
J.J.W. van der Vegt
Department of Applied Mathematics, University of Twente, Enschede, the Netherlands

Summary

Spectral elements with mass lumping allow for explicit time stepping and are therefore attractive for modelling seismic wave propagation. Their formulation on rectangular elements is straighforward, but for tetrahedra only elements up to degree 3 are known. To preserve accuracy after mass lumping, these elements require additional nodes that make them computationally more expensive. Here, we propose a new, less restrictive accuracy condition for the construction of these continuous mass-lumped elements. This enables us to construct several new tetrahedral elements. The new degree-2 and degree-3 elements require 15 and 32 nodes, while the existing ones have 23 and 50 nodes per element, respectively. We also developed degree-4 tetrahedral elements with 60, 61, or 65 nodes per element. Numerical examples confirm that the various mass-lumped elements maintain the optimal order of accuracy and show that the new elements are significantly more efficient in terms of accuracy versus compute time than the existing ones.

Topics:
1.25 Seismic Modelling;
6.03 High-performance Computing for Geoscience Applications

Main objectives:
The development of robust finite element methods with minimal computational cost for solving wave propagation problems.

New aspects covered:
We found a new accuracy condition for the development of mass-lumped elements, which led to new tetrahedral elements of degree 2 and 3 with less nodes than the existing ones and therefore significantly more efficient. We also found several new mass-lumped tetrahedral elements of degree 4.

Introduction

Spectral finite elements with mass lumping are attractive for the simulation of seismic wave propagation because they are accurate and allow for explicit time stepping. Their construction is straightforward for quadrilaterals and hexahedra, but not for triangles or tetrahedra. For the latter, mass lumping reduces the accuracy when using standard Lagrangian basis functions. Fried and Malkus (1975) showed that the accuracy can be restored by enriching the interior of the degree-2 triangular element with a bubble function—a cubic function that vanishes on all edges. Taking the product of the bubble function with higher-degree polynomials enabled the construction of triangular elements of degree 3 (Cohen et al., 1995, 2001), 4 (Mulder, 1996), 5 (Chin-Joe-Kong et al., 1999), 6 (Mulder, 2013), and 7 to 9 (Liu et al., 2017; Cui et al., 2017). In 3D, elements of degree 2 (Mulder, 1996) and 3 (Chin-Joe-Kong et al., 1999) could be constructed by augmenting the polynomial space for the basis functions with higher-degree face and internal bubble functions.

Here, we show that the accuracy requirement for the construction of those elements was too strong and that the number of auxiliary bubble functions for higher-degree tetrahedral elements can be significantly reduced. The new accuracy condition enabled us to construct new elements of degree 2 and 3 with less nodes than the known ones, as well as three new elements of degree 4. The new elements were tested on a 3-D homogeneous acoustic problem with a point source for which the exact solution is readily available. The numerical examples show that these new elements are more efficient than the current ones. We also include a more realistic elastic problem.

Method

We consider tetrahedral elements with a Lagrangian basis. Mass-lumping is done by using an inexact quadrature rule of which the quadrature points are the same as the nodes of the basis functions. For stability, it is necessary that all the weights of the quadrature rule are strictly positive. To also maintain the order of accuracy, it was required that for elements of degree p, the quadrature rule for the mass matrix is exact for polynomials up to degree $p+p'-2$ (Ciarlet, 1978), where $p' > p$ is the highest degree of the enriched basis functions.

For $p \geq 2$, however, this requirement is too strong. Instead, we derived that it is sufficient if the quadrature rule is exact for all functions in $U_e \otimes P_{p-2}$, where U_e is the element space of polynomials up to degree p enriched with higher-degree bubble functions, and P_{p-2} is the set of polynomials up to degree $p-2$.

With this new condition, we were able to construct several new mass-lumped tetrahedral elements. To describe their quadrature rules, let x_1, x_2, x_3, x_4, with $x_1+x_2+x_3+x_4=1$, be the barycentric coordinates of the element. The quadrature rules consist of basic symmetric quadrature rules of the form $\{(x_1,x_2,x_3)\}$. By this, we mean the quadrature point with barycentric coordinates x_1, x_2, x_3, and $x_4 = 1-x_1-x_2-x_3$ and all equivalent points obtained by permuting the four barycentric coordinates and taking the first 3 coordinates. For example, $\{(\alpha,0,0)\}$ denotes the twelve interior edge points that have barycentric coordinates α, 0, 0, and $1-\alpha$. Table 1 lists the 11 equivalence classes on the tetrahedron together with the number of nodes per class and a brief description.

Table 1 *The 11 equivalence classes for quadrature nodes on the tetrahedron.*

1	$\{(0,0,0)\}$	4 vertices	7	$\{(\frac{1}{4},\frac{1}{4},\frac{1}{4})\}$	centre of tetrahedron
2	$\{(\frac{1}{2},0,0)\}$	6 edge midpoints	8	$\{(\alpha,\alpha,\alpha)\}$	4 interior points
3	$\{(\alpha,0,0)\}$	12 interior edge points	9	$\{(\alpha,\alpha,\frac{1}{2}-\alpha)\}$	6 interior points
4	$\{(\frac{1}{3},\frac{1}{3},0)\}$	4 face centres	10	$\{(\alpha,\alpha,\beta)\}$	12 interior points
5	$\{(\alpha,\alpha,0)\}$	12 interior face points	11	$\{(\alpha,\beta,\gamma)\}$	24 interior points
6	$\{(\alpha,\beta,0)\}$	24 interior face points			

Table 2 *Mass-lumped finite elements. The first column contains the basic polynomial degree p of the element, the second the number of nodes n per element, the third the element space and the last the quadrature rule configuration. The older elements are marked by an asterisk.*

p	n	U_e	node pattern $\mathbf{K} = \{K_1, K_2, \ldots, K_{11}\}$
1	4*	P_1	$\{1,0,0,\ 0,0,0,\ 0,0,0,0,0\}$
2	15	$P_2 \oplus B_f \oplus B_i$	$\{1,1,0\ ,1,0,0,\ 1,0,0,0,0\}$
2	23*	$P_2 \oplus B_f P_1 \oplus B_i$	$\{1,1,0,\ 0,1,0,\ 1,0,0,0,0\}$
3	32	$P_3 \oplus B_f P_1 \oplus B_i P_1$	$\{1,0,1,\ 0,1,0\ ,0,1,0,0,0\}$
3	50*	$P_3 \oplus B_f P_2 \oplus B_i P_2$	$\{1,0,1,\ 0,2,0,\ 0,1,1,0,0\}$
4	60	$P_4 \oplus B_f P_2 \oplus B_i\big(P_2 \oplus B_f\big)$	$\{1,1,1,\ 0,2,0,\ 0,2,1,0,0\}$
4	61	$P_4 \oplus B_f P_2 \oplus B_i\big(P_2 \oplus B_f \oplus B_i\big)$	$\{1,1,1,\ 0,2,0,\ 1,2,1,0,0\}$
4	65	$P_4 \oplus B_f\big(P_2 \oplus B_f\big) \oplus B_i\big(P_2 \oplus B_f \oplus B_i\big)$	$\{1,1,1,\ 1,2,0,\ 1,2,1,0,0\}$

To describe the basis functions on the elements, let $B_f := \{x_1x_2x_3, x_1x_2x_4, x_1x_3x_4, x_2x_3x_4\}$ denote the four face bubbles, $B_i := \{x_1x_2x_3x_4\}$ the interior bubble, and define $B_fP_k := B_f \otimes P_k$, $B_iP_k := B_i \otimes P_k$. Table 2 provides an overview of the existing and new tetrahedral elements. The node pattern $\mathbf{K} = \{K_1, K_2, \ldots, K_{11}\}$ defines the number of independent nodes per equivalence class, modulo permutations. From the node pattern $\mathbf{K}$ and the specification U_e of the basis functions, we could solve for the nodal positions and quadrature weights by requiring exact quadrature for all functions in $U_e \otimes P_{p-2}$.

The new elements require less nodes. Stability analysis shows that they also allow for larger time steps.

Results

We start with an accuracy test of the old and new mass-lumped tetrahedral element methods on a constant-density acoustic model, using a structured mesh that consists of cubes divided into 6 hexahedra. The domain is $[-2,2]^3\,\mathrm{km}^3$ and the acoustic wave speed 2 km/s. A 3.5-Hz Ricker wavelet, starting from the peak, is placed at $(0,0,1000)$ m, and 78 receivers are placed on a line between $x_r = -1925$ and $x_r = +1925$ m with a 50-m interval at $y_r = 0$ m and $z_r = 800$ m. Data were recorded for 0.6 s, counting from the time at which the wavelet peaked.

The simulations were carried out with OpenMP on 24 Intel® Xeon® E5-2680 v3 cpus running at 2.50 GHz. Figure 1 shows the the observed root mean square (RMS) errors for the various schemes against the number of degrees of freedom N and against wall clock time. The latter should not be taken too literal because it depends on code implementation, compiler and hardware. It can be further reduced by going to single precision, but then it becomes more difficult to measure the errors when they become small. Therefore, we ran a double-precision version of the code when preparing these figures.

Fourth-order time stepping was used for degrees higher than one (Dablain, 1986). For degree 4, we also considered 6th-order time stepping, but the errors were nearly the same as with 4th-order time stepping for the current example.

Power-law fits show that the RMS errors converge with the optimal order $p+1$ and thus confirm that the new elements maintain their order of accuracy. Figure 1 also shows that the new mass-lumped methods require less degrees of freedom and computation time for the same accuracy. For the degree-2 methods, the difference in wall clock time is one order of magnitude, while for the degree-3 methods this difference is around a factor 2. The degree-4 methods become more efficient for errors below 10^{-3}.

We also tested the methods on the more realistic salt model from Kononov et al. (2012), made elastic by replacing the water layer at the top by rock. Figure 2 displays vertical cross sections through the 3-D vertical displacement wavefield, clipped at 10% of its maximum amplitude with red for positive and blue for negative values. Small amplitudes were replaced by the P-velocity to give an impression of the model. A vertical force source was placed on the surface at (2000,2200,0) m. The wavelet was a 12-Hz

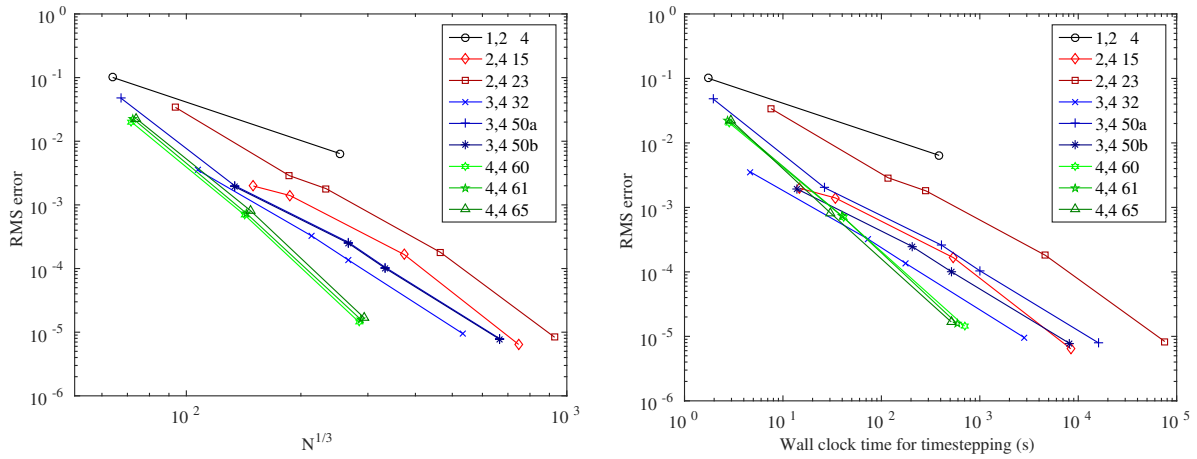

(a) (b)

Figure 1 *RMS errors as a function of the cube root of the number of degrees of freedom (a) and as a function of the wall clock time (b). The legend contains element degree, order of time-stepping scheme and the number of nodes per element. The older elements, apart from the one with degree 1, have degree 2 with 23 nodes and degree 3 with 50 nodes and two variants called a and b.*

Ricker. The top layer causes strong reverberations.

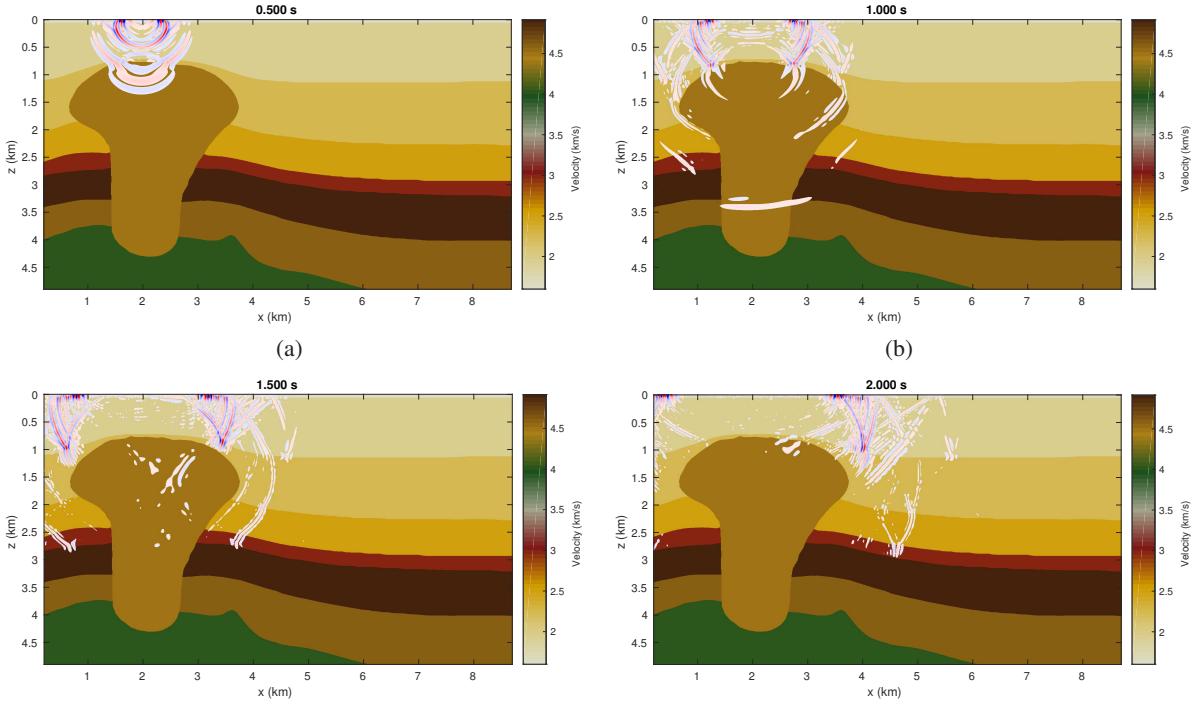

(a) (b) (c) (d)

Figure 2 *Vertical cross section at $y = 2$ km of the P-velocity with a superimposed snapshot of the vertical displacement after 0.5 s (a), 1.0 s (b), 1.5 s (c) and 2.0 s (d).*

Conclusions

We developed a less restrictive accuracy condition for the construction of continuous mass-lumped elements, which enabled us to construct several new tetrahedral elements. The new degree-2 and degree-3 tetrahedra require 15 and 32 nodes, while the current tetrahedra require 23 and 50 nodes per element, respectively. We also developed degree-4 tetrahedra with 60, 61, and 65 nodes per element. Mass-lumped tetrahedra of this degree did not exist so far. Numerical examples confirm that the new mass-lumped

methods maintain an optimal order of accuracy and show that the new elements are significantly more efficient than the existing ones. We have only considered tetrahedral elements, but the accuracy condition might also lead to more efficient triangular elements.

Acknowledgements

The first author received funding from Shell Global Solutions International B.V. for his PhD research.

References

Chin-Joe-Kong, M.J.S., Mulder, W.A. and van Veldhuizen, M. [1999] Higher-order triangular and tetrahedral finite elements with mass lumping for solving the wave equation. *Journal of Engineering Mathematics*, **35**, 405–426.

Ciarlet, P.G. [1978] *The finite element method for elliptic problems*, *Studies in mathematics and its applications*, 4. North-Holland.

Cohen, G., Joly, P., Roberts, J.E. and Tordjman, N. [2001] Higher order triangular finite elements with mass lumping for the wave equation. *SIAM Journal on Numerical Analysis*, **38**(6), 2047–2078.

Cohen, G., Joly, P. and Tordjman, N. [1995] Higher order triangular finite elements with mass lumping for the wave equation. In: G. Cohen, E. Bécache, P.J. and Roberts, J.E. (Eds.) *Proceedings of the Third International Conference on Mathematical and Numerical Aspects of Wave Propagation*. SIAM, Philadelphia, 270–279.

Cui, T., Leng, W., Lin, D., Ma, S. and Zhang, L. [2017] High order mass-lumping finite elements on simplexes. *Numerical Mathematics: Theory, Methods and Applications*, **10**(2), 331–350.

Dablain, M.A. [1986] The application of high-order differencing to the scalar wave equation. *Geophysics*, **51**(1), 54–66.

Fried, I. and Malkus, D.S. [1975] Finite element mass matrix lumping by numerical integration with no convergence rate loss. *International Journal of Solids and Structures*, **11**(4), 461–466.

Kononov, A., Minisini, S., Zhebel, E. and Mulder, W.A. [2012] A 3D tetrahedral mesh generator for seismic problems. In: *Proceedings of the 74th EAGE Conference & Exhibition*. B006.

Liu, Y., Teng, J., Xu, T. and Badal, J. [2017] Higher-order triangular spectral element method with optimized cubature points for seismic wavefield modeling. *Journal of Computational Physics*, **336**, 458–480.

Mulder, W.A. [1996] A comparison between higher-order finite elements and finite differences for solving the wave equation. In: Désidéri, J.A., LeTallec, P., Oñate, E., Périaux, J. and Stein, E. (Eds.) *Proceedings of the Second ECCOMAS Conference on Numerical Methods in Engineering*. John Wiley & Sons, Chichester, 344–350.

Mulder, W.A. [2013] New triangular mass-lumped finite elements of degree six for wave propagation. *Progress In Electromagnetics Research*, **141**, 671–692.